

# FIELD QUALITY OF THE LHC DIPOLE MAGNETS IN OPERATING CONDITIONS

L. Bottura, M. Buzio, S. Fartoukh, S. Russenschuck, S. Sanfilippo, W. Scandale, F. Schmidt, E. Todesco, L. Walckiers, R. Wolf, CERN, Geneva, Switzerland

## Abstract

We report here the main results of the field measurements performed so far on the pre-series LHC superconducting dipoles at superfluid helium temperature. After discussing the results at injection and collision conditions, we focus on the non-linear contributions at high field, on the contribution of superconductor magnetization at injection, and on ramp rate effects. The statistics accumulated on the first magnets of the production verify the hypotheses that have been used to design the correctors scheme for the LHC. In particular high field saturation is in line with the expectations, although a small systematic deformation due to Lorentz forces affects both sextupole and decapole terms. The decay at injection and snap-back at beginning of beam acceleration require careful characterization.

## 1. INTRODUCTION

The superconducting dipole magnets for the LHC must satisfy strict requirements on the produced field strength and homogeneity expressed as maximum field imperfections. Multipole errors in the superconducting magnets will affect the beam modifying critical parameters such as orbit, tune, coupling and chromaticity. The control of the main beam parameters will require active correction loops efficient only if the field errors are sufficiently known at operating conditions [1]. As the field quality at operation depends on several contributions of different physical origin, it is mandatory to pursue a detailed analysis of the measurement at cryogenic temperature in order to verify that each contribution to the magnetic field is within expected bounds. This analysis is also necessary to verify that all production steps are within the specified limits.

We have measured to date seven pre-series, twin-aperture dipoles from the three European suppliers contributing to the LHC production. Although the available statistics is limited, the measured values allow a first verification of the hypotheses made on field strength and homogeneity, and in particular on the non-linear contributions originating from the superconducting cable. In this paper we will report the measured values of field and field errors at injection and at collision conditions as compared to the beam specification [2]. We will then examine the effect of high field saturation at collision, persistent currents and field decay at injection, and eddy currents during ramps. The geometric contribution of the coil to the field, being of primary importance, is discussed in a companion paper at this conference [3].

Field errors are given in unit of  $10^{-4}$  relative to the dipole field strength at the reference radius of 17 mm.

## 2. MAIN FIELD AND MULTIPOLES

The integrated transfer function of the dipole field (ratio of integrated dipole to operating current) is plotted in Figure 1. The only bound for the integrated transfer function is related to the spread among magnets and apertures, as the average integrated dipole field strength is corrected by the current setting. The spread observed among the seven magnets tested amounts to 6.4 units at injection and 5.5 units at collision, safely within the specified r.m.s. value of 8 units. The integrated field direction in each magnet aperture shows an average twist (difference from one end to the opposite one) of 1.1 mrad, while the average co-linearity error (difference between the two apertures) is 0.5 mrad. Both values are within the specified bounds of 3 mrad for the twist and 0.8 mrad for the co-linearity.

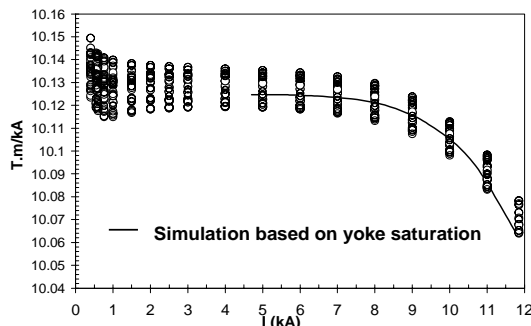


Figure 1: Integrated transfer functions measured in the pre-series dipoles as a function of the current.

Figures 2 and 3 summarise the integrated higher order multipoles as measured at collision (8.34 T) and injection (0.54 T) field and compared to the maximum allowable bounds on the average and the spread for LHC operation [2]. The boundaries are intended as the minimum and maximum value of the integrated multipoles that still allow successful correction of the errors with the foreseen correction system.

At collision field  $b_2$  and  $b_4$  were successfully minimised by changing the geometry of the iron inserts in the magnetic circuit [4]. The large  $b_3$  values are due to the difficulty to tune the coil geometry of the preseries magnets for the conflicting requests of good field quality and sufficient pre-stress.

At injection most integrated multipoles are within the allowable limits, apart for  $b_5$  that is marginally outside the specified bounds for the average and  $b_7$  that affects only

the motion of particles having betatron excursions larger than  $10\sigma$ .

Corrective actions have been taken to reduce the geometric contribution of  $b_3$  and  $b_5$  on the following magnets, as discussed in [3].

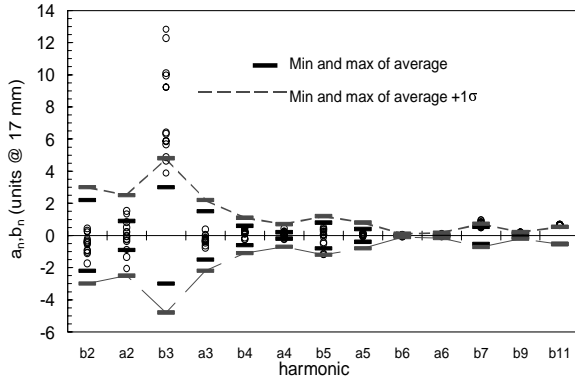


Figure 2: Integrated harmonics measured at collision compared to the specified ones [2] ( $1\sigma$  bound).

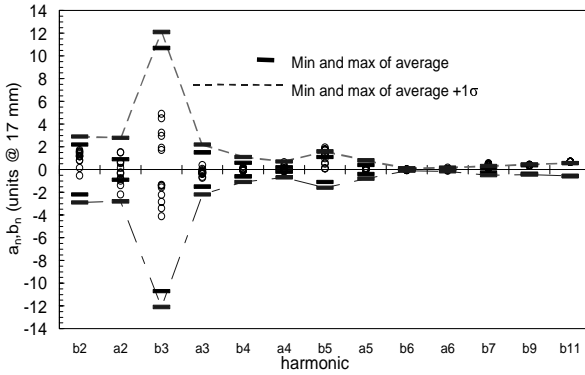


Figure 3: Integrated multipoles measured at injection field compared to the expected ones ( $1\sigma$  bound).

### 3. HIGH FIELD EFFECTS

Field strength and homogeneity at collision conditions are mostly affected by iron saturation and, as we will discuss, deformation of the coil geometry under the Lorentz force. We have defined an *effective saturation* as the difference between the multipole value at collision conditions and its geometric value, i.e. as measured at 5 kA. In Table 1 we display the measured effective saturation at nominal field and compare it to the values based on computer modelling taking into account iron saturation [5]. Only normal multipoles are reported as no effect is expected nor observed on skew multipoles.

Table 1: Saturation measured at collision field compared to expected from iron saturation.

Multipole [unit]	Average meas.	Spread meas.	Average calculated	Spread calculated
$b_1$	-56.6	1.53	-61	0
$b_2$	-1.80	0.23	-1.81	0
$b_3$	0.3	0.08	0.18	0.87
$b_4$	0.2	0.01	0.17	0
$b_5$	-0.145	0.014	0.01	0

A fair agreement is found between measurements and calculation for  $b_2$  and  $b_4$ . The discrepancy observed for  $b_3$  and  $b_5$  is likely due to the deformation induced by the electromagnetic forces. To demonstrate this effect Figure 4 indicates that the decapole ( $b_5$ ) is calculated to be marginally sensitive to the iron saturation whilst the measured values normalised to the geometric decapole at 5 kA indicates a quadratic dependence on the excitation current.

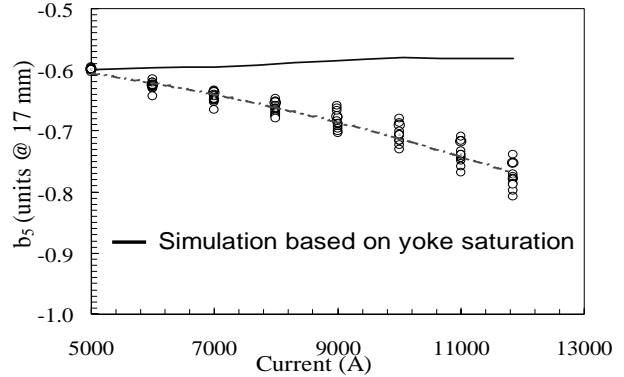


Figure 4: Variation of the normal decapole as a function of magnet current as compared to the variation expected from the iron yoke saturation

## 4. INJECTION EFFECTS

### 4.1 Persistent Currents

The most important effect to the field at injection comes from the persistent currents in the superconducting filaments of the cable. We define the *effective magnetisation* contribution as the difference between the multipole value measured once the injection current is reached and the geometric component measured at 5 kA. The measured effective magnetization broadly corresponds to the calculated persistent current contribution as shown in Table 2. The experimental data are significantly smaller than the computation in the case of the  $b_1$ ,  $b_3$  and  $b_5$  with a difference that reduces as the multipole order increases. It is thought at present that the origin of the discrepancy is the magnetization of the iron, and in particular the small but appreciable hysteresis associated with high field cycles. The details of this effect are under investigation.

Table 2: Measured effective magnetization at injection compared to expected effect from persistent currents.

Multipole [unit]	Average meas.	Spread meas.	Average calculated	Spread calculated
$b_1$	-2.19	1.78	-5.43	0.33
$b_3$	-7.31	0.31	-7.97	0.11
$b_5$	1.12	0.16	1.09	0.02
$b_7$	-0.39	0.027	-0.43	0.007

### 4.2 Ramp Rate Effects

Currents circulating between superconducting strands induce additional field errors during current ramp. This effect is proportional to the ramp rate and to the inverse of the inter-strand resistance. For the inter-strand resistance

a minimum value of  $15 \mu\Omega$  has been set as production target. Table 3 displays the inter-strand resistance values obtained from measurement of the energy loss during current cycles, and shows that this parameter is much higher than targeted. Correspondingly, the ramp rate errors measured on six dipoles are significantly smaller than expected as shown in Table 4, correlating well with the high inter-strand resistance. The data reported there are referred to a ramp starting at injection with the maximum rate of 10 A/s, corresponding to reaching 7 TeV in approximately 1000 s. These measured values are small enough to be neglected for the LHC operation.

Table 3: Inter-strand resistance as deduced from loss measurements (limit of measurement accuracy :  $100 \mu\Omega$ ).

magnet	1001	1002	2001	3001	3002
$R_c (\mu\Omega)$	60	30	70	>100	>100

Table 4 : Ramp rate induced multipoles for a nominal ramp of 10A/s at injection field (0.54 T) compared to calculated ones for an inter-strand resistance of  $15 \pm 5 \mu\Omega$

Multipole [unit]	Average meas.	Spread meas.	Average calc.	Spread calc.
$b_1$	1	0.96	5.24	1.1
$b_2$	0.022	0.046	0	1.53
$a_2$	-0.007	0.105	0	0.55
$b_3$	0.053	0.128	0.46	0.87
$a_3$	-0.012	0.021	0	0.26
$b_4$	0.009	0.013	0	0.21
$a_4$	-0.001	0.042	0	0.54
$b_5$	0.001	0.042	-0.11	0.34
$a_5$	0.001	0.009	0	0.12

### 4.3 Decay and Snap-Back

During injection at constant current excitation the field multipoles exhibit a drift with typical time scales in the order of several minutes to several hours. We report in Figure 5 the decay of  $b_3$  as measured in all magnets during a 1000 s simulated injection. Despite identical powering history the magnets behave in a significantly different manner both with respect to the magnitude and time dependence of the effect. The decay is followed by the rapid snap-back at the start of the ramp. The amplitude of the snap-back, depending on the decay, is different from magnet to magnet. We quantify the multipole decay by taking the difference between the value at the end and beginning of injection ( $t=1000$  s and 0 s in Figure 5).

Table 5: Measured multipole variation induced by the magnetisation decay observed during a plateau of 1000 s at injection field compared to the expected maximum.

Multipole [unit]	Average meas.	Spread meas.	Average expected	Spread expected
$b_2$	0.017	0.101	0.001	0.200
$a_2$	0.079	0.229	0.000	0.800
$b_3$	1.6	0.473	2.559	0.950
$a_3$	0.007	0.072	0	0.670
$b_4$	0.027	0.038	0	0.21
$a_4$	0.032	0.09	0	0.64
$b_5$	-0.304	0.107	-0.3	0.84
$a_5$	0.001	0.025	0	0.18

The measured decay for all multipoles is summarized in Table 5. As expected only systematic contributions of allowed multipoles and random variations of low order multipoles are large. The wide  $b_3$  spread between magnets in addition to the variation of the time dependence due to pre-cycling conditions will be a critical issue for the LHC operation since a systematic variation of  $b_3$  by 0.02 unit changes the accelerator chromaticity by 1 unit. Likewise,  $b_5$  must be predicted and corrected within 0.1 unit in all machine conditions to avoid a loss in dynamic aperture.

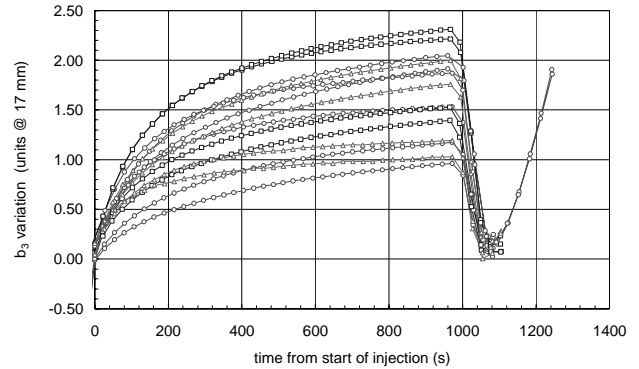


Figure 5: Decay and snap-back of the sextupole component for a plateau at injection of 1000 s.

## 5. CONCLUSIONS

The first seven pre-series twin-aperture superconducting dipole magnets for the LHC have been measured in all accelerator conditions. The yoke saturation effect appears to be broadly understood, although the measurements at high field indicate an elastic deformation of the coil originally not foreseen in the field errors budget. The hypotheses made on field effects due to the superconducting cable have been confirmed. The field errors generated by the persistent currents and their decay during the injection plateau show the largest variation from magnet to magnet. These contributions will therefore require careful consideration. The field errors caused by current ramp rate inducing inter-strand current are smaller than expected and not critical for the accelerator.

## 6. REFERENCES

- [1] O. Brüning, Accumulation and ramping in the LHC, Procs. of the workshop on LEP-SPS Performance, Chamonix, Jan. 2000, CERN-SL-2000-007 DI.
- [2] S. Fartoukh., O Brüning, Field Quality Specification for the LHC Main Dipole Magnets, LHC-Project-Report-501, Geneva, CERN, Oct. 2001.
- [3] E. Todesco, et al., Status Report on Field Quality in the Main LHC Dipoles, this conference.
- [4] S. Redaelli, et al., Optimization of the Even Normal Multipole Components in the Main Dipole of the LHC, this conference.
- [5] S. Russenschuck, The Application of the BEM-FEM Coupling Method for the Accurate Calculation of Fields in Superconducting Magnets, Springer, Electrical Engineering 82 (1999).